

• 特约稿 •

DOI:10.15961/j.jsuese.201800420

# Application and Validation of a Multi-block Constitutive Model at Landslides of the Wenchuan Earthquake

STAMATOPOULOS Constantine<sup>1</sup>, XIONG Ke<sup>2</sup>, DI Baofeng<sup>2,3\*</sup>

( 1.Stamatopoulos and Associates Limited Liability Company, 5 Isavron Street, Athens 114-71, Greece &Hellenic Open University, Parodos Aristotelous 18, Patra 26335, Greece;

2.Institute for Disaster Management and Reconstruction, Sichuan University, Chengdu 610207, China;

3.College of Architecture &Environment, Sichuan University, Chengdu 610065, China )

**Abstract:** A multi-block model and a corresponding computer program have been developed which predict the kinematics of landslides. Furthermore, a unique event for studying different models simulating the triggering and movement of landslides is the 2008 Wenchuan earthquake in the mountainous region in Sichuan Province of China, which caused a large number of rapid landslides. The purpose of the paper is two-fold: (a) to propose and incorporate into the multi-block model constitutive relations predicting soil response along slip surfaces, and (b) to apply the multi-block model with the constitutive relations at landslides triggered by the Wenchuan earthquake. The proposed constitutive equations predict the shape of the shear stress-displacement response measured in ring shear tests. In the application, four landslides caused by the Wenchuan earthquake were considered. Only in one of these landslides the shear resistance-displacement response along the slip surface has been measured in laboratory tests. At this landslide, the triggering and movement of the landslide was predicted. In the other landslides, back analyses were performed and it was observed that the multi-block model predicted reasonably well the final configuration of all slides. In addition, as the measured and back-estimated total friction angle of all landslides was less than  $18^\circ$ , and the materials along the slip surface were sandy, it is inferred that some, or all of the slip surface during these slides was sheared in an undrained manner and excess pore pressures generated during sliding played a key role in the triggering and movement of these landslides. Concluding, the paper (A) proposed and validated a multi-block constitutive model which can be applied to predict the triggering and movement of earthquake-induced slides and (B) by analyzing four landslides of the 2008 Wenchuan earthquake, it concludes that some, or all of the slip surface during these slides, was sheared in an undrained manner and excess pore pressures generated during sliding played a key role in the triggering and movement of these landslides.

**Key words:** Wenchuan earthquake; multi-block model; seismic displacement; landslides; back analysis; strain softening

中图分类号: X43

文献标志码: A

文章编号: 2096-3246(2018)03-0033-13

As a result of the disastrous 12th May 2008 Wenchuan earthquake, a large number of rapid landslides which traveled over very large distances were triggered in the mountainous Wenchuan County, Sichuan Province of the People's Republic of China<sup>[1-4]</sup>. This makes the event unique for studying different models simulating the

triggering and movement of landslides.

The sliding-block model<sup>[5]</sup> is frequently used to simulate movement of landslides triggered by earthquakes<sup>[6]</sup>. This model is generally successful in estimating small ground deformations without loss of strength. However, when the ground deformations are large, this

收稿日期:2018-03-13

基金项目:The National Key R&D Program of China (2017YFC1502903); Sichuan International Cooperation and Exchange for Science and Technology (2016HH0079); "Novel methodologies for the assessment of risk of ground displacement" under ESPA 2007-2013 of Greece; under action: Bilateral S & T Cooperation between China and Greece

作者简介:STAMATOPOULOS Constantine(1962—), male, director & instructor, PhD. Research direction: Disaster prevention and risk assessment model. E-mail: [K.stam@saa-geotech.gr](mailto:K.stam@saa-geotech.gr)

\* 通信联系人 E-mail: [dibaofeng@scu.edu.cn](mailto:dibaofeng@scu.edu.cn)

model is not accurate, primarily because of (a) changes of geometry of the sliding mass towards a gentler inclination<sup>[7]</sup> and (b) loss of strength in saturated soils along the slip surface<sup>[8]</sup>. Regarding the effect (a) above, it is caused by the law of physical equilibrium where masses move towards a more stable configuration. Regarding the effect (b) above, ring shear devices where sandy samples can be sheared under undrained conditions have recently been developed and applied to study the response of saturated sands along slip surfaces<sup>[9-10]</sup>. These tests illustrate the considerable decrease in the soil strength at large shear displacement, which may occur due to the generation of excess pore pressures. In particular, the measured shear stress-displacement response of these tests illustrates: First, the shear stress ( $\tau$ ) gradually increases from its initial value with shear displacement ( $u$ ) at a decreasing rate, until the peak shear stress is reached. At the peak shear stress, the rate of change ( $d\tau/du$ ) is zero. Then, for saturated soils exhibiting strain softening, as  $u$  increases further,  $\tau$  decreases to its residual value, while ( $d\tau/du$ ) (1) first decreases from zero until a limit displacement value reached, then (2) it starts to increase, and finally (3) at very large shear displacement it tends to zero.

This study aims to provide an easy-to-use and cost-effective methods predicting the triggering and displacement of earthquake-induced slides. The paper, after describing the multi-block model, proposes and implements at the multi-block model constitutive equations describing the response above and applies it to landslides occurred during the Wenchuan earthquake. In the application, four landslides of the Wenchuan earthquake were considered because in only these landslides their kinematics was similar to what the multi-block model predicts. From these landslides, only in one of these landslides the shear resistance-displacement response along the slip surface has been measured in laboratory tests. At this landslide, the triggering and movement of the landslide was predicted. In the other landslides, back analyses were performed using the multi-block model. Conclusions are drawn regarding the ability of the multi-block model to predict the triggering and movement of landslides. Last but not least, the soil resistance measured in the ring shear tests and obtained in the back analyses performed is discussed and is related to a possible mechanism of the triggering and excessive movement of

these landslides.

## 1 The multi-block model

This section describes briefly the multi-block model<sup>[3]</sup> (Fig. 1) proposed by Stamatopoulos and Di<sup>[11-13]</sup>. It utilizes previous work by Sarma<sup>[14]</sup>, Ambraseys and Srbulov<sup>[15]</sup>, Stamatopoulos<sup>[16]</sup>, Sarma and Chlimentzas<sup>[17]</sup>. A general mass sliding on a slip surface which consists of  $n$  linear segments is considered. In order for the mass to move, at the nodes between the linear segments of the slip surface, interfaces inside the sliding mass are formed, where resisting forces are exerted. Thus, the mass is divided into  $n$  blocks sliding in different inclinations. Soil is assumed to behave as a Mohr-Coulomb material at both the slip surface and at the interfaces.

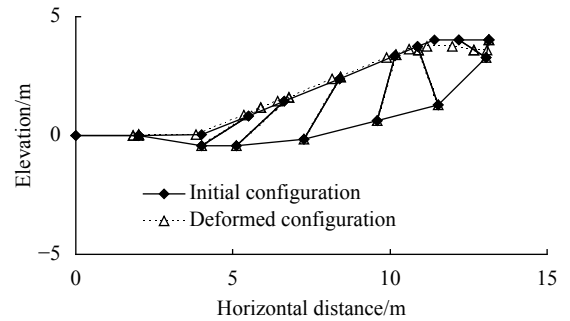


**Fig. 1 Multi-block method: Typical initial and deformed configuration**

When the slide moves and the blocks are not separated, the velocity must be continuous at the interfaces. This rule predicts that the relative displacement of the  $n$  blocks is related to each other as:

$$du_i/du_{i+1} = \cos(\delta_i + \beta_{i+1}) / \cos(\delta_i + \beta_i) \quad (1)$$

Where  $u_i$  is the displacement along the linear segment  $i$  of the trajectory,  $d$  refers to increment, the subscripts  $i$  and  $i+1$  refer to trajectory segments  $i$  and  $i+1$  counting uphill and  $\beta_i$  and  $(90-\delta_i)$  are the inclinations of the trajectory segment and interface  $i$ , respectively.

Taking equilibrium for each block, and summing up the equations, the governing equation of the sliding system can be obtained. When a horizontal component of acceleration  $a(t)$  is applied, the governing equation of motion has the following form:

$$du_n^2/dt^2 = A(a(t) - a_c), \text{ for } du_n/dt > 0 \quad (2)$$

Where  $A$  is a factor and  $a_c$  is the critical horizontal acceleration which is just sufficient for movement of the sliding mass. The factors  $A$  and  $a_c$  depend on the geometry, the mass, the pore water pressure prior to shearing and

the frictional and cohesive resistance at the base and the interfaces of the  $n$  blocks.

As shear displacement develops, the masses and lengths of each block, and thus the factors  $A$  and  $a_c$  in equation (2) also change. The transformation rule, which states that when each block is displaced by  $d\tilde{u}_i$ , each point of the block is also displaced by  $d\tilde{u}_i$ , is applied. As the internal interfaces are fixed in space, at each increment, cross-sectional area with width  $du_i$  is transferred from body ( $i$ ) to body ( $i-1$ ) according to equation (1). The deformation which this rule predicts is illustrated in Fig. 1.

A computer program which solves equation (2) has been developed. The factors  $A$  and  $a_c$  are time dependent and thus are updated at each increment in the numerical analysis. Output of the program includes the initial and final slide geometries and acceleration velocity and displacement of nodes of the sliding mass versus time.

## 2 Constitutive equations, implementation and computer program

In the case where the initial stress ratio  $\tau_o/\sigma'_o$  equals zero, we propose the following equation which simulates the soil response described in the introduction section:

$$\tau = \sigma'_o R \quad (3)$$

Where

$$\text{For } u_1 > u > 0, \quad R = (R_{\text{res}}/r) [1 - (1 - u/u_1)^{a_1}] \quad (4)$$

$$\text{For } u > u_1, \quad R = R_{\text{res}} + b(u+a)^{(1-n)} [(n-1)u - (n-2)u_1 + a] \quad (5)$$

Where

$$b = R_{\text{res}}(1/r - 1)(a + u_1)^{n-2} \quad (6)$$

Where  $R_{\text{res}}$ ,  $r$ ,  $u_1$ ,  $a_1$ ,  $a$ ,  $n$  are the six model parameters. During unloading-reloading of applied shear load, the model assumes that zero shear displacement develops. In the case where the initial stress ratio  $\tau_o/\sigma'_o$  equals to  $R_o$ , the displacement is  $u'$  and equals to:

$$u' = u - u_o, \quad u' > 0 \quad (7)$$

Where  $u$  is given by equations (4)~(6) and, according to equations (3)~(6)

$$u_o = u_1 \left[ 1 - (1 - rR_o/R_{\text{res}})^{1/a_1} \right] \quad (8)$$

We define  $u_a$  as the  $u$  value where  $d^2R/du^2 = 0$  and the parameter  $a_2$  as

$$a_2 = u_a/u_1 \quad (9)$$

Next, according to equations (7)~(8)

$$a_2 = (a/u_1 + n)/(n-1) \quad (10)$$

It is inferred that, we can replace the model parameter  $a$  of equations (3)~(6) with the parameter  $a_2$ , which, unlike the parameter  $a$  has physical meaning: i.e. it is directly associated with  $u_a$ . The parameter  $a$  of equations (3)~(6) can be obtained from the parameter  $a_2$ , as

$$a = u_1 [a_2(n-1) - n] \quad (11)$$

As illustrated in Fig. 2, from a given shear stress-displacement curve measured in a shear device, determination of the model parameters  $R_{\text{res}}$ ,  $r$ ,  $u_1$ ,  $a_2$  is straightforward: the parameter  $R_{\text{res}}$  is the stress ratio  $R$  of the material at the residual (final) state. The parameter  $r$  is the ratio of the maximum stress ratio of the shear stress-displacement response ( $R_{\text{max}}$ ) and  $R_{\text{res}}$ . The parameter  $u_1$  gives the shear displacement at  $R_{\text{max}}$ . The parameter  $a_1$  determines the rate of change of the shear stress with shear displacement at the interval  $u < u_1$ . The parameter  $a_2$  gives the shear displacement ( $a_2u_1$ ) at  $u > u_1$  when  $d^2R/du^2 = 0$ . Also, the parameter  $n$  determines the rate of change of the shear stress with shear displacement at the interval  $u > u_1$ . The effect of the parameters  $n$ ,  $a_2$  in the shear stress-displacement response is illustrated later in section 7.

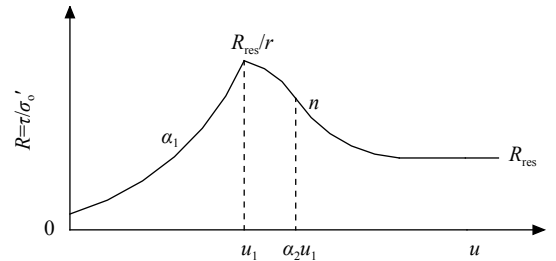


Fig. 2 Graphical illustration of the constitutive model of equations (3)~(6)

The advantage of the proposed model is its simplicity and its small number of parameters. However, it has the disadvantage of generality. When applying this model along slip surface segments, tests with similar relative density, confining stress and initial shear stress as existing in-situ should be used to estimate the model parameter.

Finally, it can be noted that the residual friction angle of the material ( $\varphi_{\text{res}}$ ) equals  $\text{atan}(R_{\text{res}})$ . Furthermore, under undrained conditions, the parameter  $R_{\text{res}}$  is related to the total excess pore water pressure generated during shaking ( $P$ ), and the effective residual friction angle of

the material ( $\varphi'$ ):

$$R_{\text{res}} = \tan \varphi' (1 - P/\sigma'_o) \quad (12)$$

At this point it should be noted that undrained conditions occur during fast shearing when the water table line is above the slip surface, as a result e.g. of precipitation due to a recent rainfall. Thus, assuming, for example that as a result of undrained shearing  $P/\sigma'_o$  equals 0.5, it is inferred that  $R_{\text{res}}$  is 50% less under undrained than under drained conditions.

The constitutive equations (3)~(11) were coupled with the multi-block model described above by varying only the friction angle at the base of each block  $i$ ,  $\varphi_i$ , as

$$\varphi_i = \arctan(\tau_i/\sigma'_{o-i}) \quad (13)$$

In equation (13),  $\tau_i$  and  $\sigma'_{o-i}$  are the shear stress and the initial (prior to slide movement) effective normal stress at the base of block  $i$ , respectively. It should be noted that the values of  $\tau$ ,  $u$  and  $\sigma'_o$  of equations (3)~(6) correspond to  $\tau_i$ ,  $u_i$  and  $\sigma'_{o-i}$  in equation (13). In the computer program associated with the multi-block model described above, soil strength along the slip surface is simulated either by the Mohr-Coulomb law, or by the constitutive equations (3)~(11). In the second case, at each increment, the values of  $\tau_i$  are updated in terms of the incremental shear displacement.

### 3 Application procedure of the multi-block model along slip surfaces and very large displacement

In the case that the slip surface is not pre-existing, application of the multi-block model first requires the prediction of the location of the slip surface by stability analysis. A stability method relevant to the multi-block sliding mass geometry has been developed by Sarma and Tan<sup>[18]</sup>. However, the study of the ability of stability methods in order to estimate the location of this slip surface is beyond the purpose of the present work.

In order to apply the multi-block model along pre-defined slip surfaces under earthquake loading, the steps needed are: (a) to define the trajectory, ground and water table surfaces, (b) to obtain the constitutive model parameters from results of laboratory tests, (c) to obtain the interface angles and (d) to predict the triggering and displacement of the slide by applying the multi-block model with the constitutive model at the slip surface for a representative seismic motion.

Regarding step (b) for slip surface or trajectory segments consisting of saturated sand, the model parameters of equations (3)~(6) must be obtained from undrained ring shear, or equivalent, tests on soil samples with the same relative density as in-situ and consolidated at the same confining stress and initial shear stress as that existing in-situ. For slip surface segments consisting of dry soil, the model parameters of equations (3)~(6) must be obtained from drained shear tests, or, if such tests do not exist, from strength values based on effective stresses.

Regarding step (c), if the inclinations of the interfaces are not predefined according to existing faults, they are obtained according to the condition of minimum critical acceleration value at the initial slide configuration. However, at large deformations, estimation of the interslice angles of the sliding mass according to the condition of minimum critical acceleration at the initial slide configuration may not be adequate. This is resolved by applying the criterion of minimum critical acceleration not only at the initial, but also at the final slide configuration and taking the average values at the common interfaces of the two configurations. The final slide configuration can be obtained by applying the multi-block model assuming that the interface angles which are not defined at the initial slide configuration equal zero. In particular, for both the initial and final slide configurations the following procedure is used to obtain the interface angles: Estimate the interface angle of the first node,  $\delta_1$ , assuming that the interfaces of the other nodes ( $\delta_2, \delta_3, \dots, \delta_n$ ) equal zero, under the condition of minimum critical acceleration value. Along the slip surface the residual values of soil strength are used, as it is the most representative of the soil strength during motion. At the interfaces, peak values of strength are used. The reason is that as the internal interfaces are fixed in space, they are continuously reforming with new material and thus the strength cannot be at residual<sup>[15]</sup>. Next, estimate the remaining  $\delta_i$  values by using the  $\delta_{i-1}, \dots, \delta_1$  values previously obtained and assuming  $\delta_{i+1}, \dots, \delta_n = 0$ . Repeat the above procedure starting from the  $\delta_i$  values obtained in the previous iteration until the new set of  $\delta_i$  values does not differ from the previous, and thus convergence is achieved.

The application procedure described above can be used to predict seismic displacement of landslides. Furthermore, the residual soil strength of past landslides can

be estimated using the iteration procedure described in Tab. 1, where the first value of the residual soil shear strength adopted in the procedure are also given. Di present graphical illustration of an approximate procedure to obtain the trajectory of past landslides from their initial and final configurations<sup>[3]</sup>. It should be noted that each application of the multi-block model in Tab. 1 lasts only a few seconds.

**Tab. 1 Proposed manner to apply the multi-block model to back-estimate the residual friction angle mobilized during past landslides**

Step No	Description
1	$\delta_i = 0$
2	Find the $\varphi$ value along the slip surface, which predicts the measured slide displacement $(u_1 + u_n)/2$ within 5%. Start with $\varphi$ equal to the average slope inclination.
3	Using the $\varphi$ value obtained in step 2, estimate all the interface angles $\delta_i$ at the initial slide configuration according to the procedure of section 3.
4	Using the $\varphi$ value obtained in step 2, obtain the final slide configuration using the multi-block model. Then, estimate all the interface angles $\delta_i$ at the final slide configuration according to the procedure of section 3.
5	Using the average $\delta_i$ values of steps 3 and 4 using the procedure described in section 3.
6	Compute the landslide displacement using the multi-block model with the $\delta_i$ values selected in step 5. Compare the computed displacement under step 6 with the measured.
7	In the case that more than 5% percent difference exists between the measured and computed under step 6 displacement, estimate a new $\varphi$ value and corresponding landslide displacement by performing again steps 2~6 steps.

## 4 Landslides triggered by Wenchuan earthquake

Wenchuan earthquake occurred in the Longmen mountain, which is located on the eastern boundary area of the Tibetan plateau and is one of the most significantly deformed regions in China, where earthquakes occur frequently. The Wenchuan earthquake occurred on the Yinxiu-Beichuan fault of the Longmen mountain, which extends from Dujiangyan to Guangyuan (Fig. 3). On the southeast side of the fault alternating strata of sandstone, shale, mudstone and colluvial materials, derived from the above rocks exist<sup>[19]</sup>. Climate of the region is typically humid subtropical monsoon, with plentiful rainfall.

The multi-block model of Fig. 1 can be applied only in landslides which move as rigid bodies in one dimension. At this point is should be noted that rigid motion

does not occur when fluid-like motion occurs, which is related to movement of saturated soil and thus water table line near the ground surface. Furthermore, movement in one dimension occurs in homogenous geological settings, where ground properties do not change with horizontal location.

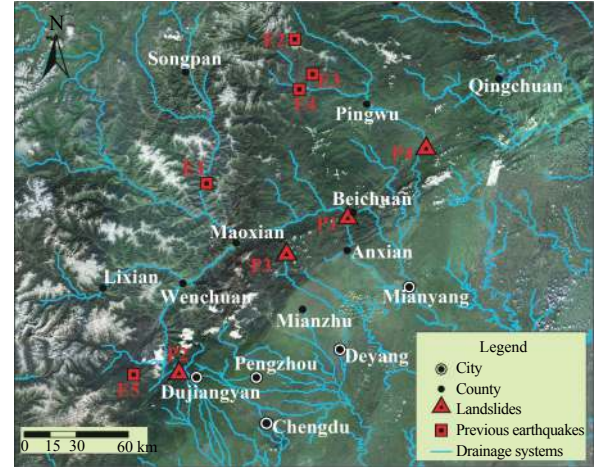


**Fig. 3 Location map of the past landslides studied (symbol Pi) and of previous earthquakes (symbol Ei)**

The bibliography was carefully studied and Fig. 3 shows the location of all past landslides triggered by the Wenchuan earthquake, found in the bibliography (symbol Pi) where (a) their initial and final cross-sectional geometries are well-documented and (b) moved as rigid bodies in one dimension, and thus the multi-block model of Fig. 1 can be applied. They are four in number and Tab. 2 gives their names and the relevant references. It can be observed that all landslides are located in the same mountain range, namely near the Yinxiu-Beichuan fault. In addition, it can be observed that landslides are located near rivers. According to the above discussion it can be inferred that although the four landslides are separated by one or two hundred kilometers near the Yinxiu-Beichuan fault, they have the common characteristics of (a) homogenous geological setting and (b) water table line near the slip surface, not near the ground surface.

**Tab. 2 Typical landslides triggered by the Wenchuan earthquake**

Slide No	Name	Reference	Comment
P1	Niumiangou	[20]	—
P2	Tangjiashan	[21]	—
P3	Zhengjiashan	[22]	—
P4	Donghekou	[4],[19]	Ring shear tests have been performed along the slip surface

In only one of these landslides, the Donghekou slide, ring shear tests were performed on representative samples retrieved from the slip surface. Tab. 3 gives the date, epicenter location and magnitude of severe earthquakes which have occurred in the vicinity of the landslides ( $M > 5.2$ , Distance  $< 250$  km), retrieved from [www.earthquaketrack.com]. The epicenter of the earthquakes is mapped in Fig. 3 (symbol Ei), except from the earthquake E2, which is located beyond the range of the map. Section 5 below validates the proposed model by predicting the triggering and displacement of the Donghekou slide, while section 6 validates the proposed model by back analyses of the other landslides.

**Tab. 3 The date, epicenter location and magnitude of the Wenchuan earthquake and previous severe earthquakes in the region**

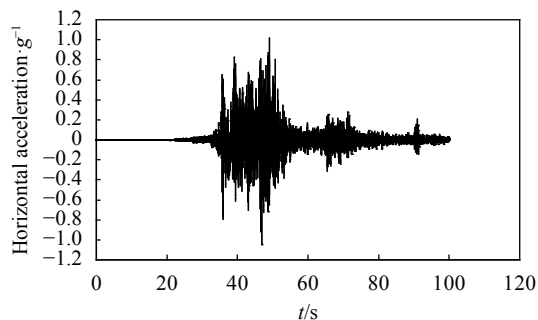
No	Coordinates	Date	$M$
E1	32.0,103.700	25/8/1933	7.5
E2	32.752,104.157	16/8/1976	6.9
E3	32.571,104.249	21/8/1976	6.4
E4	32.492,104.181	23/8/1976	6.7
E5	31.002,103.322	12/5/2008	7.9

## 5 Application of the multi-block constitutive model in a case where soil resistance has been measured along the slip surface

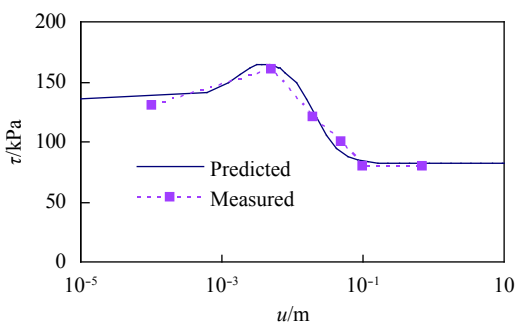
The cross-section of the initial and final slide configurations of the Donghekou landslide, the only one of the landslides of Tab. 2 where soil resistance has been measured along the slip surface, is given by [4]. As the earthquake occurred before rainy season and there was no rain prior to and during the earthquake, the water table was not presumably near the ground surface. By using an advanced ring shear apparatus, tests have been carried out by Sun<sup>[4]</sup> to study the response of the saturated soil along the slide slip surface under the loading that was actually applied during the earthquake<sup>[3]</sup> (Fig. 4(a)). The sample has particle size  $D_{50}=0.01$  mm, practically zero plasticity and was sheared with  $\sigma'_o=300$  kPa and  $\tau_o=90$  kPa. Fig. 4(b) presents the measured shear stress-displacement response of this test<sup>[4]</sup>.

At first, the geometry of the slide is represented. As shown in Fig. 5(a) the trajectory is represented by 6 nodes where the 4 nodes correspond to the slip surface at the initial configuration. Nodes determining the slip sur-

face (and trajectory) and the ground surface are given with different symbols. The initial location of the ground surface is represented by 4 additional nodes. As mentioned earlier, the water table line most probably was not considerably above the slip surface and is assumed to coincide with the slip surface in the analyses.

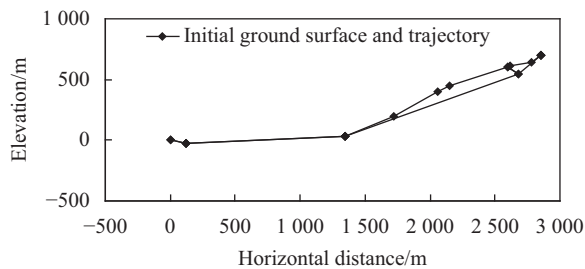


(a) Wenchuan earthquake typical motion near the epicenter

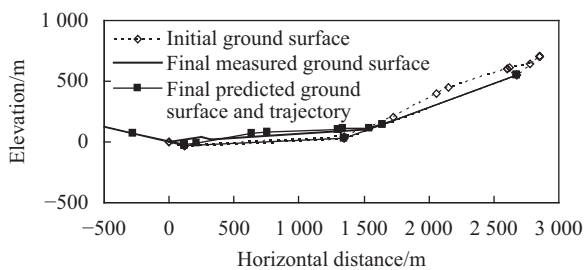


(b) Measure and prediction of shear stress-displacement response

**Fig. 4 Shear stress-displacement response of the Donghekou landslide**



(a) Simulation of the initial slide configuration with the multi-block model



(b) Measured and computed final slide geometry

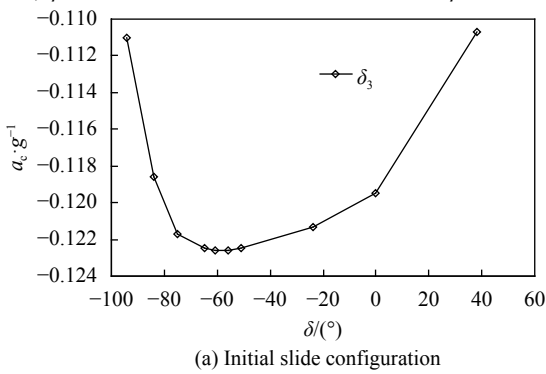
**Fig. 5 Measured and computed slide geometry of the Donghekou slide**

Next, the model parameters of the constitutive model are obtained by the prediction of the relevant shear tests. Tab. 4 gives the set of parameters of the constitutive equations (3)~(6) which predict the test. Fig. 4(b) compares model predictions of the constitutive model with the measured response. Good agreement can be observed. In addition, the peak total friction angles values, used in the interfaces in the analyses, are obtained:  $\varphi_{\max} = 30^\circ$ , according to the peak total strength value measured in the ring shear tests.

**Tab. 4 Constitutive model parameters which fit the laboratory tests of Fig. 5(b)**

$R_{\text{res}}$	$r$	$u_1/m$	$a_1$	$a_2 u_1/m$	$n$
0.22	0.5	0.008	2	0.016	8

In order to estimate the interface angles of the sliding mass of the slides according to the method described in section 3,  $\varphi = 30^\circ$  is used at the interfaces and  $\varphi = 15^\circ$



along the slip surface. At this point it should be reminded that the response of the proposed method for the evaluation of the interface angles is identical to the classical Mohr-Coulomb criteria. Fig. 6 gives the critical acceleration in terms of the interslice angles at the initial slide configuration obtained according to the method described in section 3. The indices of the interslice angles 1~3 give the corresponding node, counting from left to right, and denoting as “0” the node at horizontal distance 0 m. After that, the final slide configuration is obtained by applying the multi-block model with the friction angles given above and assuming that the interface angles not defined at the initial slide configuration are equal to zero. According to Fig. 6, the average obtained interslice angles to be used in the computations below were  $\delta_1 = -9^\circ$ ,  $\delta_2 = -38^\circ$ ,  $\delta_3 = -56^\circ$ .

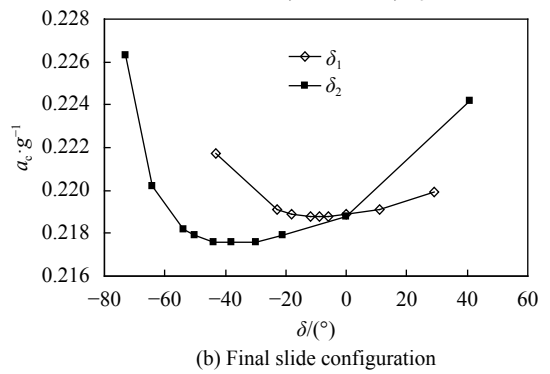


**Fig. 6 Computed critical acceleration of the Donghekou slide in terms of the interslice angles**

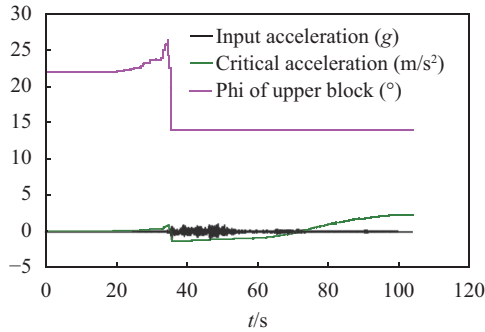
Once the interface angles are obtained, the initial geometry of the slide is completely defined (Fig. 5(a)) and the multi-block model with the constitutive model along the slip surface is applied. The constitutive model parameters which are given in Tab. 4 are being used. At the interfaces, the same peak soil strength as used to obtain the interface angles is being used. In order to demonstrate conservatively that the proposed model predicts the triggering mechanism, the representative input signal was applied with the maximum absolute acceleration value in the downward direction. As this is applied, Fig. 7 gives the input acceleration and the computed (a) critical acceleration and equivalent friction angle (given by equation (13)) of the upper block and (b) the velocity (V), and the distance moved of the upper block (u), all in terms of time. Fig. 8(b) gives the computed final slide configuration. The measured final slide configuration is

also given for comparison.

Fig. 7 illustrates that, as the earthquake is applied, some shear displacement accumulates. This causes the friction angle at the base of the blocks to increase. Once the peak friction angle is reached, due to material softening, the friction angle decreases drastically, to its residual value, at  $t = 33$  s. At this point, the critical acceleration of the sliding system is negative (this means that the slide is unstable) and the slide velocity starts to increase and displacement to accumulate rapidly. As the slide moves, the mass slides at a progressively smaller average inclination. The critical acceleration of the sliding mass gradually increases and it becomes positive at  $t = 70$  s. After that, the slide velocity starts to decrease, and becomes zero at  $t = 105$  s. At this point, the slide stops. The maximum slide velocity is 48 m/s.

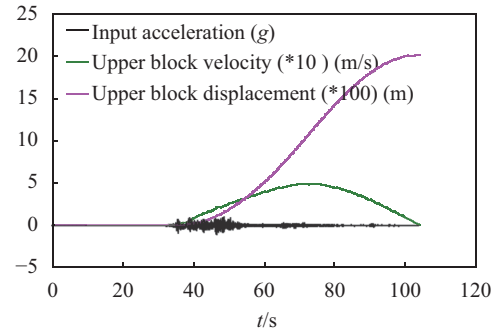
Parametric analyses were performed, where the in-

put acceleration decreased by 50%. Again, the landslide triggering was predicted and the landslide displacement



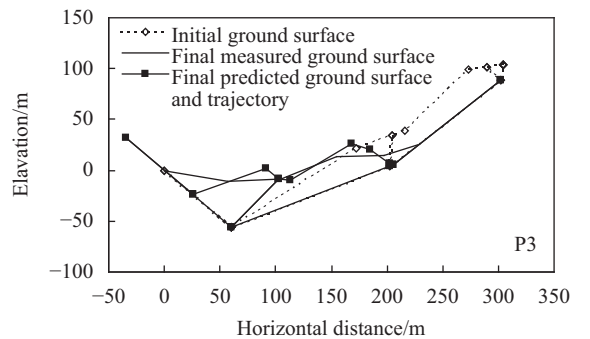
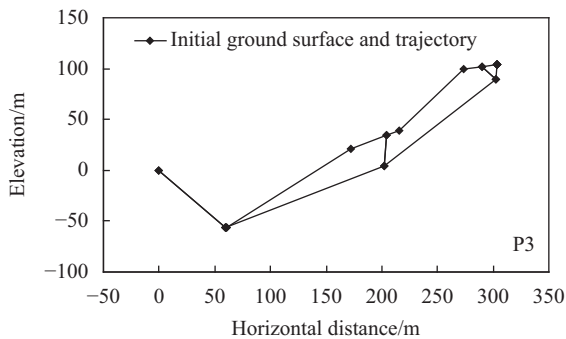
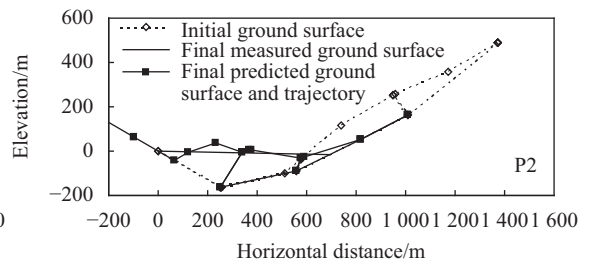
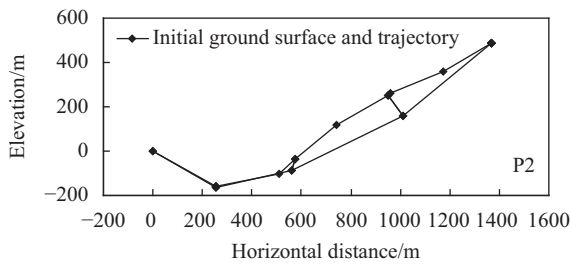
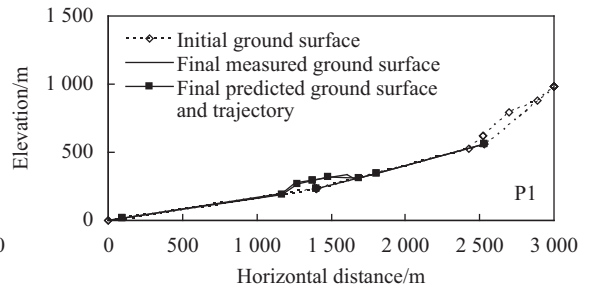
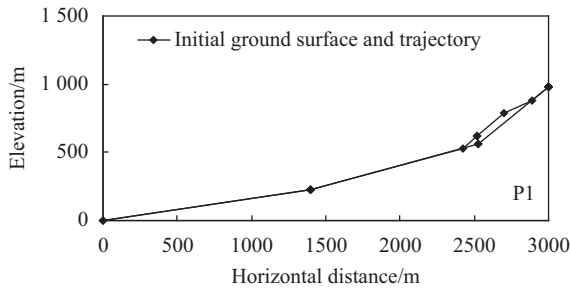
(a) Critical acceleration and equivalent friction angle (given by equation (13)) of the upper block

was modified by less than 10%, as landslide movement is affected primarily by the residual soil strength.



(b) Velocity and the distance moved of the upper block

**Fig. 7 Input acceleration and computed of the Donghekou slide, all in terms of time**



(a) Simulation of the initial slide configuration with the multi-block model

(b) Measured and computed final slide geometry

**Fig. 8 Measured and computed slide geometry of landslides P1,P2,P3**

Above, it was demonstrated that in the relevant seismic event the proposed method predicts the triggering of the landslide. However, in order to make full verification, below it is confirmed that the proposed method also predicts the non-triggering in other seismic events. For the main seismic events which have occurred in the vi-

city of the landslide of Tab. 3, the attenuation relation proposed by Chen predicts an  $a_{\max}$  value in the location of the landslide less than  $0.1g$ <sup>[23]</sup>. Application of the model with the input acceleration of Fig. 4(a) normalized such as  $a_{\max}=0.1g$  illustrated that, similarly to in-situ, the landslide was not triggered and displacement was less than a



few mm.

### 6 Application of the multi-block model in a case where soil resistance has not been measured along the slip surface

The iteration back analysis procedure of Tab. 1 was applied in the landslides P1~P3 of Tab. 2. In these landslides, first, the trajectory and the initial ground surface of each landslide were simulated by linear segments, as given in Fig. 8. Water table elevation is not available at the cross-sectional configurations of the slides. As the earthquake occurred in May, just at the start of the annual rainfall season and as just prior to or during the earthquake it did not rain, the water table was not presumably near the ground surface. For the above reasons, in these runs the water table line was assumed not to be above the slip surface and the trajectory. The interface friction angle was taken as 35° in all cases. The reason is that 35° is a typical value of the peak friction angle of dry material with a LL value less than 25%<sup>[24]</sup>. Tab. 5 gives the obtained residual friction angle value and, addition-

ally, the time duration of motion of these slides. It also gives the obtained interslice angles. The indices of the interslice angles give the corresponding node of the trajectory, counting from left to right, and denoting as “0” the node at horizontal and vertical location 0 m. The initial geometry of the slides is given in Fig. 8(a) and Fig. 8(b) gives the computed final slide geometries. Fig. 9 gives the computed critical acceleration in terms of the interslice angles for (a) the initial slide configuration and (b) the final slide configuration. The indices of the interslice angles 1~4 give the corresponding node, counting from left to right, and denoting as “0” the node at horizontal.

**Tab. 5 Back analysis of past landslides. The residual friction angle and time duration of motion obtained per past landslide (run 1). The corresponding average values of the interface angles obtained at the initial and final slide configurations, used in the analyses**

Slide No	$R_{res}$	$t/s$	$\delta_1$	$\delta_2$	$\delta_3$
P1	18	72	-10	-24	—
P2	16	29	29	17	-33
P3	15	13	42	5	-43

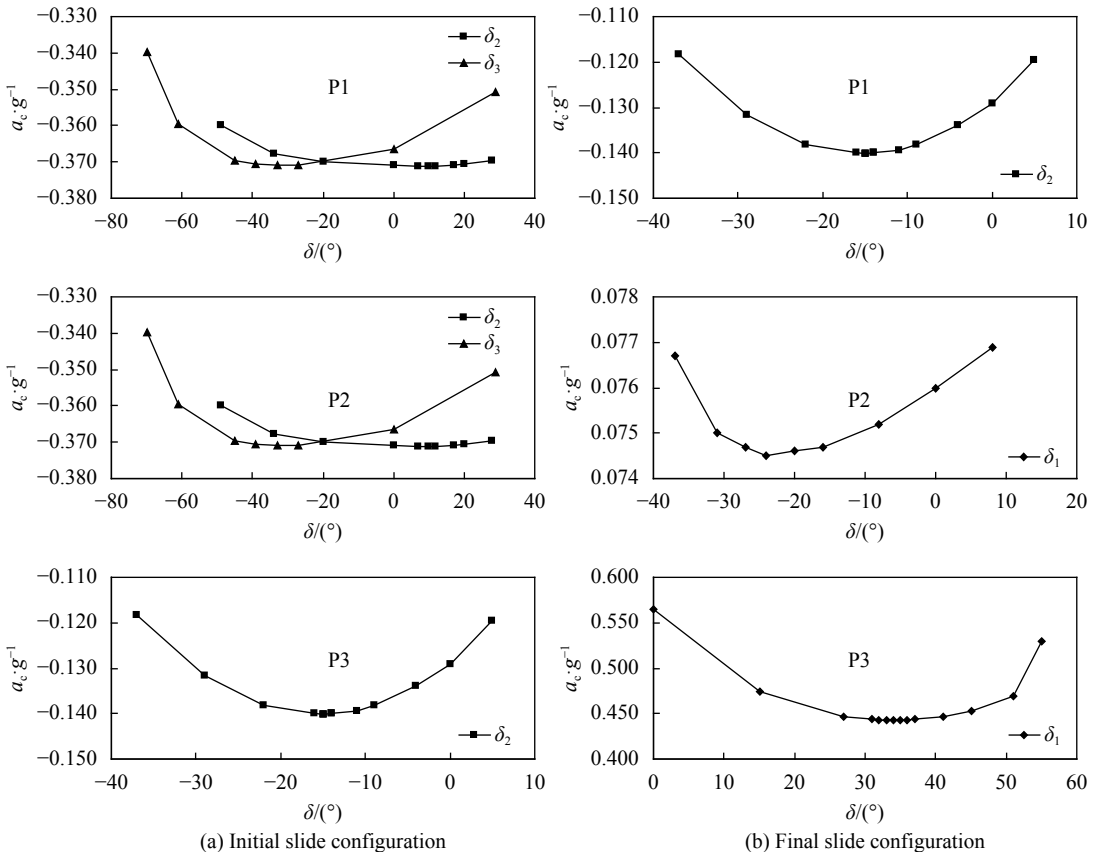


**Fig. 9 Computed critical acceleration of landslides P1, P2, P3 in terms of the interslice angles**

## 7 The constitutive equations (3)~(6) and its effect on the triggering of the landslides

It is of interest to study the relationship between the prediction results and the values of the parameters of the constitutive model. Fig. 10 presents the effect of the model parameters  $n$  and  $a_2u_1$  on the constitutive model given by equations (3)~(6), while all the other model parameters are as given in Tab. 4. Cases 1~4 correspond to  $(n, a_2u_1) = (2.5, 0.01), (10, 0.01), (2.5, 0.02), (10, 0.02)$  respectively. All the other model parameters are as given in Tab. 4. (a) in logarithmic scale, (b) in natural scale. Furthermore, parametric analyses were performed

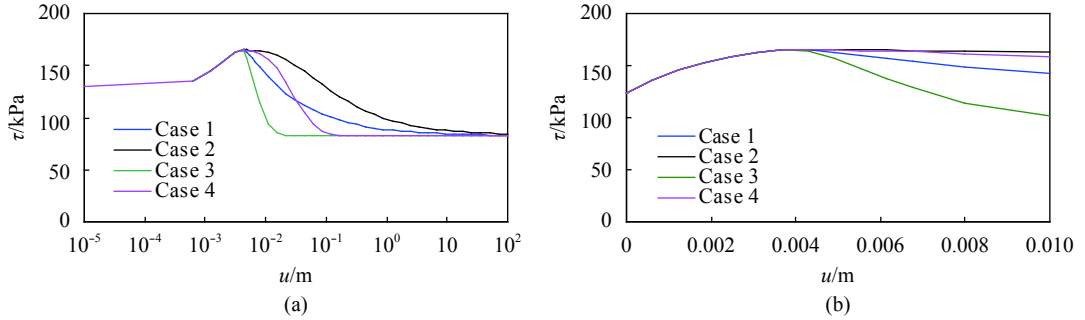


Fig. 10 Parametric analyses of the constitutive model given by equations (3)~(6). Cases 1~4 are described in the text

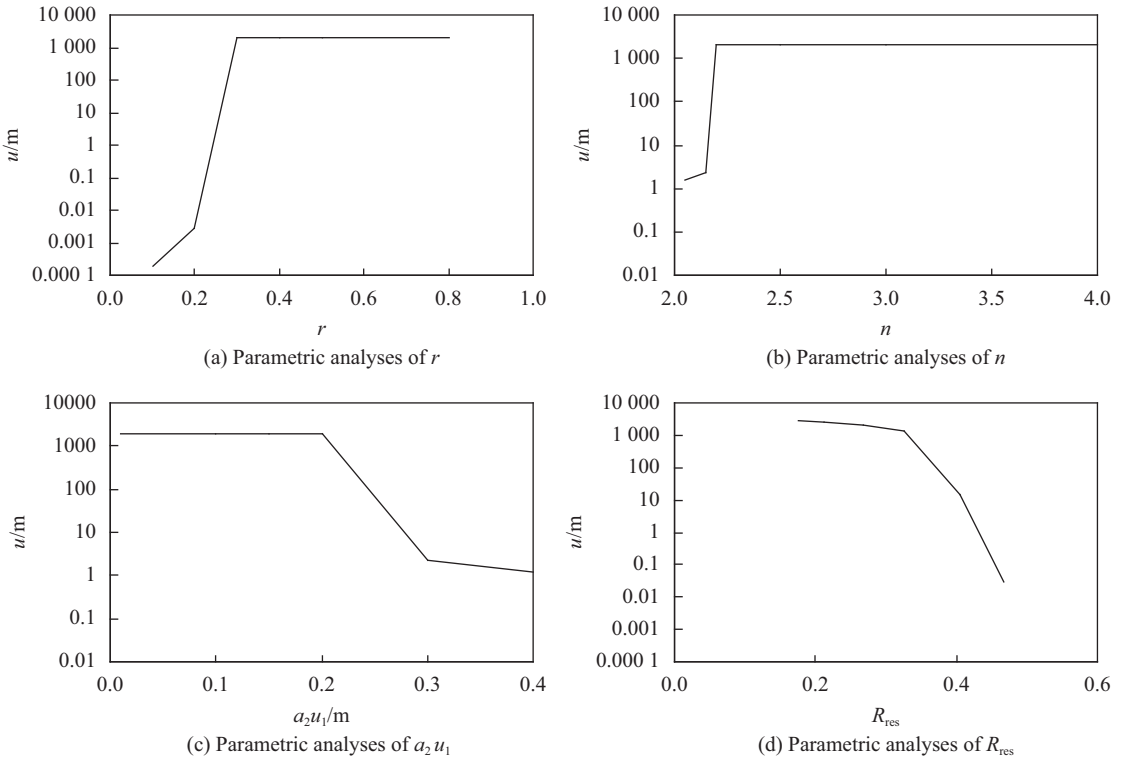


Fig. 11 Parametric analyses of the effect if the constitutive model parameters on the seismic displacement of the Donghekou landslide

In addition, it is of interest to investigate the relationship between the past severe earthquakes in Tab. 3

where the effect of the parameters of the constitutive model on the seismic displacement of the Donghekou landslide was studied. First it was observed that the parameters  $a_1$  and  $u_1$  (for value  $a_2u_1$  less than the value of 0.016 m of Tab. 4) do not affect the displacement. Then, Fig. 11 gives the effect if the constitutive model parameters (a)  $r$ , (b)  $n$ , (c)  $a_2u_1$  on the seismic displacement of the landslide. All the other model parameters are as given in Tab. 4. It can be observed that landslide triggering is affected by all these parameters, while once triggering occurs, the landslide displacement is affected as a first approximation only by the parameter  $R_{res}$ .

and the four landslides. Regarding the Donghekou landslide, this was studied in section 5. Regarding the land-

slides P1~P3 of Tab. 2, for the earthquakes E1~E4 of Tab. 3, the attenuation relation proposed by Chen<sup>[23]</sup> predicts an  $a_{\max}$  value in their location less than 0.1g. Application of the constitutive equations (3)~(6) with the  $R_{\text{res}}$  value of Tab. 5 and the remaining model parameters of Tab. 4 illustrated that in all landslides P1~P3 (a) for the seismic motion of Fig. 4(a) triggering occurs, while (b) for the seismic motion of Fig. 4(a) normalized at  $a_{\max}=0.1g$  triggering does not occur and the seismic displacement is only a few mm. The above, under the assumption that the model parameters  $a_1$ ,  $r$ ,  $u_1$ ,  $n$ ,  $a_2$  of Tab. 4 measured at landslide P4 can be applied for landslides P1~P3 also, predicted triggering of landslides P1~P3 at the seismic event E5, and non-triggering at the events E1~E4.

## 8 Discussion

### 8.1 Performance of the multi-block model

The multi-block model and the associated proposed procedure performed satisfactorily in this work. In particular, regarding the estimation of the interface angles with the criterion of the minimum critical acceleration, convergence existed in all cases. This is illustrated in Fig.6 and Fig.9. Regarding the prediction of the actual measured slide response, the computed time duration of motion (Fig.8(b), Tab. 5) agrees with the observed rapid occurrence of the landslides. In addition, the predicted final configuration of all slides reasonably agrees with the measured ones. Last but not least, landslide triggering was predicted at the seismic event E5 of Tab. 3, and non-triggering at the events E1~E4.

### 8.2 Triggering mechanism of the landslides of the Wenchuan earthquake

Chang and Zhang indicate that the soil along the slip surface of the landslides of the Wenchuan earthquake consisted primarily of sands and silts with Liquid Limit (LL) value less than 25%<sup>[25]</sup>. Such soils under dry conditions exhibit a residual friction angle greater than 25°<sup>[24]</sup>. As the measured or the back-estimated total residual friction angle of all four landslides, was less than 18°, it is inferred that part, or all of the slip surface, was sheared in an undrained manner and the generation of excess pore pressure reduced the total friction angle of the material. The manner in which the total residual friction angle is reduced by the generation of excess pore pres-

ures is given by equation (12). It is inferred that due to the humid climate of the region, the saturation of soils along the slip surface caused the generation of excess pore pressures during the seismic excitation of the Wenchuan earthquake, which played a key role in the triggering of the catastrophic landslides.

## 9 Conclusions

The work first proposes and incorporates into a recently-proposed multi-block model the constitutive relations which predict the shape of the shear stress-displacement response measured in ring shear tests. Then, it applies the multi-block model with constitutive equations along the slip surface at four landslides triggered by the Wenchuan earthquake. The following were observed:

Only in one of these landslides the shear resistance-displacement response along the slip surface has been measured in laboratory tests. At this landslide, the triggering and movement of the landslide was predicted by the multi-block model with constitutive equations.

In the other landslides, back analyses were performed where the multi-block model predicted reasonably well the final configuration of all slides.

In all cases considered, the multi-block model predicted the rapid occurrence of the landslides.

As the measured and back-estimated residual friction angle in all landslides was less than 18°, and the materials along the slip surface have a Liquid Limit value less than 25%, it is inferred that some, or all of the slip surface during these slides, was sheared in an undrained manner.

## References:

- [1] Di B F, Chen N S, Cui P, et al. GIS-based risk analysis of debris flow: an application in Sichuan, southwest China[J]. *International Journal of Sediment Research*, 2008, 23(2):138–148.
- [2] Di B F, Zeng H J, Zhang M H, et al. Quantifying the spatial distribution of soil mass wasting processes after the 2008 earthquake in Wenchuan, China: A case study of the Longmenshan area[J]. *Remote Sensing of Environment*, 2010, 114(4):761–771.
- [3] Di B F, Stamatoopoulos C A, Dandoulaki M, et al. A method predicting the earthquake-induced landslide risk by back

- analyses of past landslides and its application in the region of the Wenchuan 12/5/2008 earthquake[J].*Natural Hazards*, 2017,85(2):903–927.
- [4] Sun P, Wang F W, Yin Y P, et al. An Experimental study on the mechanism of rapid and long run-out landslide triggered by wenchuan earthquake[J].*Seismology and Geology*, 2010,32(1):98–106.
- [5] Newmark N M. Effects of earthquakes on dams and embankments[J].*Geotechnique*, 1965,15(2):139–160.
- [6] Ambraseys N N, Menu J M. Earthquake-induced ground displacements[J].*Earthquake Engineering & Structural Dynamics*, 2010,16(7):985–1006.
- [7] Stamatopoulos C A. Sliding system predicting large permanent co-seismic movements of slopes[J].*Earthquake Engineering and Structural Dynamics*, 1996,25(10):1075–1093.
- [8] Whitman R V. Predicting earthquake-caused permanent deformations of earth structures[C]// Predictive Soil Mechanics. London: Thomas Telford, 1993:729–741.
- [9] Sassa K, Fukuoka H, Scarascia-Mugnozza G, et al. Earthquake-induced landslides: Distribution, motion and mechanisms[J].*Soils & Foundations*, 2014,54(4):544–559.
- [10] Wang G, Sassa K, Fukuoka H, et al. Experimental study on the shearing behavior of saturated silty soils based on ring-shear tests[J].*Journal of Geotechnical & Geoenvironmental Engineering*, 2001,133(3):319–333.
- [11] Stamatopoulos C. Correction for geometry changes during motion of sliding-block seismic displacement, ASCE[J].*Journal of Geotechnical and Geoenvironmental Engineering*, 2011,137(10):926–938.
- [12] Stamatopoulos C A, Di B F. Simplified multi-block constitutive model predicting earthquake-induced landslide triggering and displacement along slip surfaces of saturated sand[J].*Soil Dynamics & Earthquake Engineering*, 2014,67:16–29.
- [13] Stamatopoulos C A, Di B F. Analytical and approximate expressions predicting post-failure landslide displacement using the multi-block model and energy methods[J].*Landslides*, 2015,12(6):1–7.
- [14] Sarma S K. Stability analysis of embankments and slopes[J].*Geotechnique*, 1973,105(GT12):1511.
- [15] Ambraseys N, Srbulov M. Earthquake induced displacements of slopes[J].*Soil Dynamics & Earthquake Engineering*, 1995,14(1):59–71.
- [16] Stamatopoulos C A, Velgaki E G, Sarma S K. Sliding-block back analysis of earthquake-induced slides[J].*Soils & Foundations*, 2008,40(6):61–75.
- [17] Sarma S K, Chlimintzas G O. Co-seismic & post-seismic displacements of slopes[C]// XV ICSMGE Satellite conf on Lessons Learned from recent Earthquakes, 2001. Doi:10.13140/2.1.2547.8083
- [18] Sarma S K, Tan D. Determination of critical slip surface in slope analysis[J].*Geotechnique*, 2006,56(8):539–550.
- [19] Wang G H, Huang R Q, Chigira M, et al. Landslide Amplification by liquefaction of runout-path material after the 2008 Wenchuan (M 8.0) Earthquake, China[J].*Earth Surface Processes & Landforms*, 2013,38(3):265–274.
- [20] Zhou J, Su Z, Yang X. Kinetic friction coefficient and mass movement process of large rock avalanches triggered by the wenchuan earthquake[M]// Earthquake-Induced Landslides. Berlin: Springer Berlin Heidelberg, 2013:521–528. Doi:10.1007/978-3-642-32238-9\_55
- [21] Luo G, Hu X, Gu C, et al. Numerical simulations of kinetic formation mechanism of Tangjiashan landslide[J].*Journal of Rock Mechanics and Geotechnical Engineering*, 2012,4(2):149–159.
- [22] Xu Q, Zhang S, Dong X J. Genetic types of large-scale landslides induced by the wenchuan earthquake[M]// Earthquake-Induced Landslides. Springer Berlin Heidelberg, 2013:511–520. Doi:10.1007/978-3-642-32238-9\_54
- [23] Chen L. Ground motion attenuation relationships based on Chinese and Japanese strong motion data[D] Pavia: Istituto Universitario di studi superiori, 2008.
- [24] Bolton M D. The strength and dilatancy of sands[J].*Geotechnique*, 1986,36(2):219–226.
- [25] Chang D S, Zhang L M. Simulation of the erosion process of landslide dams due to overtopping considering variations in soil erodibility along depth[J].*Natural Hazards & Earth System Sciences*, 2010,10(4):933–946.



Dr. Constantine Stamatopoulos has a PhD in Civil Engineering from Massachusetts Institute of Technology, 1989. As a partner of the firm, Dr Stamatopoulos has been principal-in-charge for more than a hundred geotechnical engineering projects, concentrating primarily on investigations, design re-

commendations, and supervision of construction of hydroelectric plants, transportation systems, earth fill dams, harbour and offshore facilities, industrial developments, and high-rise buildings of a total value of billions of dollars. Dr Stamatopoulos has also experience with administrative liaison with the Greek Ministry, having coordinated four Greek research projects. He is the author of two books, chapters in four books, 24 papers in scientific journals. He is the author of two books, chapters in

four books, 23 papers in scientific international journals and more than 70 papers in international conferences. Also, as collaborating scientific personnel at Hellenic Open University, from the start of the Master course "Dynamics of soils and foundations" in 2004 has prepared the textbooks for the course, has taught it and supervised MS theses. In total he has taught the course for 13 years and was the supervisor for 18 MS theses. Main research interests: (a) Develop methods and models predicting earthquake-induced ground displacement, (b) develop a method mitigating liquefaction risk by preloading, (c) develop the multi-block model predicting the triggering and movement of landslides, (d) develop constitutive equations predicting the soil resistance along slip surfaces at very large ground displacement.

(编辑 张 琼)

引用格式: Stamatopoulos Constantine, Xiong Ke, Di Baofeng. Application and validation of a multi-block constitutive model at landslides of the wenchuan earthquake[J]. Advanced Engineering Sciences, 2018, 50(3): 33-45. [Stamatopoulos Constantine, Xiong Ke, Di Baofeng. Application and validation of a multi-block constitutive model at landslides of the wenchuan earthquake[J]. 工程科学与技术, 2018, 50(3): 33-45.]